

Iron Ore 2017

Paper Number: 72

The Dynamic Adhesion of Wet and Sticky Iron Ores onto Impact Plates

M. Carr¹, K. Williams², W. Chen³, B. Hayter⁴, A. Roberts⁵ and C. Wheeler⁶

1.
PhD Candidate, Centre for Bulk Solids and Particulate Technologies, Newcastle Institute for Energy and Resources, The University of Newcastle, Callaghan Australia 2308. michael.j.carr@newcastle.edu.au
2.
Associate Professor, Centre for Bulk Solids and Particulate Technologies, Newcastle Institute for Energy and Resources, The University of Newcastle, Callaghan Australia 2308. ken.williams@newcastle.edu.au
3.
Research Associate, Centre for Bulk Solids and Particulate Technologies, Newcastle Institute for Energy and Resources, The University of Newcastle, Callaghan Australia 2308. w.chen@newcastle.edu.au
4.
Undergraduate Mechanical Engineer, Department of Mechanical Engineering, The University of Newcastle, Callaghan Australia 2308. brodie.hayter@gmail.com
5.
Founding Director, Centre for Bulk Solids and Particulate Technologies, Newcastle Institute for Energy and Resources, The University of Newcastle, Callaghan Australia 2308. alan.roberts@newcastle.edu.au
6.
Associate Director, Centre for Bulk Solids and Particulate Technologies, Newcastle Institute for Energy and Resources, The University of Newcastle, Callaghan Australia 2308. craig.wheeler@newcastle.edu.au

ABSTRACT

Current trends into the mining of iron ore has seen an increase into the exploitation of problematic ore bodies that would be typically disregarded in the past. These bulk materials cause problems within all facets of the material handling stream, from remains left in train wagons to transfer chute blockages, which can cause the costly downtime of mining operations (Roberts, 1998). These problematic bulk materials are referred to as Wet and Sticky Material (WSM) due to the adhesive and cohesive nature they possess. These characteristics can be computationally expensive to model and with the development of Discrete Element Modelling (DEM) in conjunction with the advancement in computational power over the past decade, it is now more feasible to model WSMs into the DEM technique.

This research will couple two different contact models that can represent the characteristics of a WSM. These models include the Simplified Johnson-Kendall-Roberts (SJKR) and the EASO liquid bridging contact models. The SJKR contact model is an expanded form of the classic Hertz model. This model includes the tensile forces which are in the contact zone between two bodies when they are separated, which the Hertz model failed to capture (Johnson, Kendall and Roberts, 1971). The EASO liquid bridging contact model, accounts for the capillary effects and surface tension that will form between two bodies, such as that of a WSM (Soulié et al., 2006). Both of these models were coupled to give the best representation of a WSM, which was simulated using LIGGGHTS (Kloss and Goniva, 2010) as the software platform.

Additionally, this research also investigated the adhesion of problematic iron ore samples onto impact plates under dynamic conditions. An experimental setup consisting of an apron feeder and inclined impact plate was utilised, to gain an understanding of the way the material builds-up and the possible modes of failure that could be experienced. This was undertaken for different wall liner materials, wall liner angles and moisture contents of the iron ore samples. From this, a series of DEM calibration simulations were conducted on the experimental setup and particle size distributions (PSD) of the iron ore samples. This enabled forming of a database of parameters, which can be scaled for on-site applications in relation to geometry of the plant and PSDs that would represent run of mine ores.

INTRODUCTION

The increasing demand for the extraction of iron ore has called for more efficient systems that can transport the bulk material from mine site where they are typically distributed to processing plants, power stations or export terminals. This increased demand has called for the exploitation of ore bodies which would be typically disregarded and avoided in the past. These ore bodies, which are defined as wet and sticky material (WSM), may be found near or even below the water table where increasing moisture and clay content will result. WSMs are prone to cause problems in all phases of the materials handling streams. This can be from remains left in train wagons, the clogging of screens, to chute build-up, among others, which can cause the costly downtime of mining operations (Roberts, 1998 and Connelly, 2011). The additional handling costs due to downtime and sub-optimal running conditions for systems with WSMs has been shown in the range of 4 to 6 AUD per tonne (Long, 2009). This would naturally be an area of concern financially for the mining industry and measures must be set in place to increase the likelihood of these systems performing effectively.

WSMs are problematic within the material handling stream due to the inter-particle and boundary cohesion and adhesion forces. Adhesion is defined as the attraction force between differing molecules, whereas cohesion will be the attraction force between similar molecules. In the field of bulk material handling, adhesion can be defined as the tensile force for particle-to-particle and particle-to-wall contact of the bulk material, whilst cohesion is the shear resistance for particle-to-particle and particle-to-wall contact under zero normal stress (Hering, Martin and Stroher, 1989). It has been further established (Burbaum, 2009), that adhesion will only be of interest within bulk material handling for ores that also have cohesive characteristics. These bulk materials that show both characteristics are able to cause blockages within a material handling system and are typically defined as a WSM.

The bonding mechanisms of adhesion and cohesion of bulk materials can be distinguished by the occurrence of material bridges between the attracting partners (Rumpf, 1958). These bonding mechanisms, however, can occur with or without material bridges. The material bridges described by (Rumpf, 1958), can have the form of a liquid, solid or solidified liquid. Within the bulk materials handling sector, a WSM will typically have higher moisture content in comparison to free flowing ores. This higher moisture will lead to an increased adsorption layer of water that will surround the particles of the bulk material (Essington, 2003). With an increasing adsorption layer of water surrounding the particles, the formation of a liquid bridge can occur. Within a liquid bridge, the governing adhesion forces can be attributed to the capillary effects, interfacial forces and surface tension (Rumpf, 1958).

For the successful implementation of a WSM into the discrete element modelling (DEM) technique, new contact models must be investigated. Currently the DEM technique can accurately model dry free flowing materials such as gravels and other coarse granular materials. DEM does this by incorporating the rolling friction and wall friction coefficients into the well-defined Hertz contact model. However, as WSMs have higher moisture content, the contact mechanism becomes much more complex as the effect of surface tension between two particles, due to various bonding forces, starts to emerge (Burbaum, 2009). These effects will not only apply additional bonding forces between the particles, but will also alter the frictional properties of the particles and walls, which in effect, changes the flow characteristics of the bulk material (Katterfeld, Donohue and Chen, 2013).

With the expansion of computation power, it is currently more feasible to use DEM for the contact models required to describe the adhesion and cohesion mechanisms that will encapsulate the behavioural traits that WSMs show. Two contact models will be coupled in this research, that aim to describe the characteristics that wet and sticky bulk materials will show in practice. An experimental setup to identify the adhesion of problematic iron ore samples onto impact plates under dynamic conditions will also be undertaken. From this, a series of DEM calibration simulations will be conducted on the experimental setup and particle size distributions (PSD) of the iron ore samples. From this, a database of parameters can be formed which can be scaled for onsite applications in relation to geometry of the plant and PSDs that would represent Run of Mine (ROM) iron ore.

DISCRETE ELEMENT MODELLING OF WSM

To encapsulate a WSM into the DEM technique, new contact models must be investigated. The following section will introduce two different models, simulated using LIGGGHTS (Kloss and Goniva, 2010) as the software platform. It is then proposed to couple both models, where it is anticipated that a much more realistic representation of a WSM will be obtained.

Liquid Bridging Models

The formation of a liquid bridge between either particle-to-particle or particle-to-wall contact can be attributed to the capillary forces that are formed due to the surface tension of the medium in the liquid bridge (Rumpf, 1958). Models have been developed to determine the capillary force present within a liquid bridge in relation to the total energy of the bridge (Israelachvili, 1992 and Rabinovich, Esayanur and Moudgil, 2005). These models described the capillary force well, however, they only consider particles of the same diameter. To consider the effects of uneven sized particles, a model has been developed by Soulié et al., 2006, as indicated in FIG 1.

This model assumes particles that will be spherical and smooth where the surface roughness has been neglected. The liquid bridge formed is in the pendular state, which is assumed to be relatively small where the affects due to gravity are neglected. Additionally, the capillary force is analysed in a quasi-state configuration, where the viscosity of the liquid is not considered (Soulié et al., 2006). To determine the capillary force, first the volume of the liquid bridge must be determined, which is given as:

$$V = \int_{x_{c1}}^{x_{c2}} y^2(x) dx - \frac{1}{3} \pi R_1^3 (1 - \cos \delta_1)^2 (2 + \cos \delta_1) - \frac{1}{3} \pi R_2^3 (1 - \cos \delta_2)^2 (2 + \cos \delta_2) \quad (1)$$

where:

R_1 and R_2 are the particle radii.

δ_1 and δ_2 are the half filling angles.

x_{c1} and x_{c2} are the distances from y-axis to edge of liquid bridge.

In addition, the inter-particle distance, D , is given as:

$$D = R_2(1 - \cos \delta_2) + x_{c2} + R_1(1 - \cos \delta_1) - x_{c1} \quad (2)$$

From the geometry presented above in FIG 1, the capillary force acting within a liquid bridge between two particles of different size can be calculated when the surface tension, σ , is known. This is given as:

$$F = \pi \sigma \sqrt{R_1 R_2} \left[c + \exp \left(a \frac{D}{R_2} + b \right) \right] \quad (3)$$

where:

$$a = -1.1 \left(\frac{V}{R_2^3} \right)^{-0.53} \quad (4)$$

$$b = \left(-0.148 \ln \left(\frac{V}{R_2^3} \right) - 0.96 \right) \theta^2 - 0.0082 \ln \left(\frac{V}{R_2^3} \right) + 0.48 \quad (5)$$

$$c = 0.0018 \ln \left(\frac{V}{R_2^3} \right) + 0.078 \quad (6)$$

θ is the contact angle of liquid bridge.

The model presented above has recently been incorporated into the DEM technique. This model has been implemented in LIGGGHTS DEM package (CFDEM, 2016), which is referenced from the work of (Soulié et al., 2016), where different sized particles are considered for both particles that will be in contact. This contact model essentially adds a liquid bridge force that will be caused by a surface liquid film on the particles. The model can also solve for the transfer of surface liquid from one particle to another, however, dynamic conditions for the breakup of the liquid film are yet to be considered. It is appropriate to identify that when a breakup of the liquid bridge occurs, it is assumed that the surface liquid will distribute evenly between the two particles. The current state of this model also indicates that the surface liquid is assumed to be small and will have no effect on the particle mass, diameter and density (CFDEM, 2016). The current implementation of this contact model into the LIGGGHTS (Kloss and Goniva, 2010) source code, only considers particle-to-particle contact. To account for wall effects, the following section will briefly introduce the SJKR contact model where the coupling of both models was undertaken as part of this research.

Energy Based Model

The Simplified Johnson-Kendall-Roberts (SJKR) contact model (Johnson, Kendall and Roberts, 1971), is an expansion to the well-defined contact model that was investigated by Hertz, 1896. The classical Hertz contact theory provides for the elastic deformation of bodies in contact. Hertz theory, although verified experimentally, neglected to incorporate the effects of both cohesion and adhesion. This could be attributed to the Hertz model only incorporating the compressive forces and neglecting the tensile forces that can be experienced in the contact zone between two bodies when they are separated.

The experimental work of Roberts and Kendall (Johnson, Kendall and Roberts, 1971) showed that for lower loads between the particles, the contact areas between these bodies were significantly higher than those predicted by Hertz. As the loads were reduced towards zero, the additional contact forces became increasingly important, which formed the basis of the SJKR model. FIG 2 shows a schematic of the SJKR contact model for both particle-to-particle and particle-to-wall scenarios of the contact areas.

The contact radius, R_p , of particle-to-particle and particle-to-wall as described by the SJKR model is given as:

$$a_o^3 = \frac{R_p}{K} \left[F_n + \frac{3}{2} W \pi d + \sqrt{3 \pi W d F_n + \left(\frac{3 \pi W d}{2} \right)^2} \right] \quad (7)$$

where: F_n is the external normal force acting on the particle.

W is the thermodynamic work of adhesion per area unit.

R_p is the radius of the particle.

K is the composite Young's Modulus.

The work of adhesion (W) is determined as the surface energies of the two contact partners and the interfacial energy:

$$W = \gamma_1 + \gamma_2 - \gamma_{1,2} \quad (8)$$

where: γ is the surface energy of the particle.

It is appropriate to identify that when the work of adhesion is zero, ($W=0$), equation 7 will revert to the simple Hertz equation $a_0^3 = R_p F_n / K$. Finally, for the SJKR model to be implemented into the DEM technique, two main parameters need to be considered. These include the radius of the particle and the cohesion/adhesion energy density found within the contact region. The cohesion/adhesion energy density is given as a constant numerical parameter for the energy needed to separate the contact and has units (J/m^3). A simplified version of equation 7 that will use the cohesion/adhesion energy density can be given as:

$$F_{SJKR} = F_n + \Omega A_{cont} \quad (9)$$

where: Ω (J/m^3) is the cohesion/adhesion energy density.

$A_{cont} = \pi(R_p^2 - R^2)$ is the contact area.

The above model has been examined in this paper using the DEM software LIGGGHTS (Kloss and Goniva, 2010). From this, the adhesion energy density (AED) for particle-to-wall contact was coupled with the EASO liquid bridging model for particle-to-particle contact to gain a better representation of a WSM into the DEM technique.

EXPERIMENTAL SETUP

To experimentally relate the coupled numerical model above, it was necessary to design and assemble an experimental apparatus that can be used for testing. The experimental setup consisted of an apron feeder and impact plate attached to bending beam load cells to gain a quantitative analysis of the impact force. The apron feeder had a velocity of 8.5 metres per minute and was held constant for this research. Additionally, the impact height remained constant at 1.8 metres. A picture of the experimental setup can be seen in FIG 3 below.

With the experimental setup complete, it is appropriate to set a list of variables to be tested to identify the parameter sets for problematic ores. These variables can be classified into two categories: assessable and constant. The identified variables are presented in TABLE 1 below.

For the variables that have been deemed assessable, in TABLE 1, a defined set of experiments can be undertaken. The set of parameters chosen included, three iron ore samples, namely Ore A, B and C, three moisture contents for each iron ore sample and impact angles ranging from 30 degrees up to 60 degrees in five degree increments. In addition, four wall lining materials were tested which consisted of, hardened steel, polished welded overlay steel, rough welded overlay steel and ceramic tiles. To control the material mass flow

rate, a number of factors are incorporated into the testing procedure. As stated previously, the conveyor velocity was held constant of 8.5 metres per minute. In addition, a consistent burden profile was utilised for each test to ensure a uniform flow rate during experiments was maintained. This was achieved by marking a 2.2 metre by 0.2 metre rectangle directly onto the conveyer belt. Once the experimental phase of the research had been completed a series of DEM calibration simulations were conducted to see the validity of the coupled contact model to the experimental results. The DEM contact model coupling and parameter settings that were used in this research will be described in the following section.

DEM SETUP

To encapsulate a WSM into the DEM technique, it is first necessary to identify the source code that required for modelling to commence. From this, the parameter sets can be identified and iterated to gain a full calibration database, which can be scaled for on-site applications in relation to geometry of the plant and PSDs that would represent run of mine ores. The following section will outline the contact model and parameter set that was utilised.

Previous work undertaken by Carr et al., 2016, showed that for WSMs, liquid bridging contact models were a better qualitative representation compared to energy based methods for particle-to-particle contact. The model that was utilised in this particular research has been developed from the analytical work of Rabinovich, Esayanur and Moudgil, 2005. This model assumes spherical particles of constant diameter which modelled the material well, however, the wall effects were not captured to what would be experienced in reality. Conversely, energy based models were also analysed where the particle-to-wall contact showed promising results when qualitatively compared to experimental results.

To develop a better representation of a WSM into the DEM technique, a hybrid model was developed by combining two sets of source code in LIGGGHTS (Kloss and Goniva, 2010). The source codes that were utilised, included the EASO model for particle-to-particle contact and the SJKR model for particle-to-wall contact. By using the EASO model spherical particles of different diameters could be analysed. Although this model does not consider particle-to-wall contacts, creating a hybrid model with the SJKR contact model will enable for the addition of adhesion energy density to include wall effects. The parameter sets needed for this hybrid model will be discussed in the following section.

Parameter Settings

For a series of calibration simulations to be undertaken, parameter sets and limits need to be defined. The hybrid model that has been developed has four parameter sets which need to be iterated. These include, the surface tension, adhesion energy density, particle-to-particle friction and rolling friction. It is appropriate to identify that the surficial moisture content surrounding the particles and the wall friction was held constant. FIG 4 below, shows a calibration flow chart for the DEM technique which is applicable to scale models and the geometry and PSD range that will be found on-site.

To define the thresholds that will govern the numerical representation of a WSM of interest, calibration simulations for the PSD utilised in the experiments can be undertaken. The calibration tests, as indicated FIG 4, will include a shear box simulation and an inclined plate simulation. These simulations will define the

threshold for the surface tension found in the liquid bridge between particles and the maximum adhesion energy density between the particles and wall. The shear box calibration method has a square box that is filled with particles and once filled a wall is removed, where the resulting angle once the material has finished discharging is recorded. The maximum threshold for surface tension is found once no material is found to discharge. Similar for the inclined plate calibration method, a layer of particles is filled into a cylinder onto a wall liner which is then rotated 180 degrees. The maximum threshold for adhesion energy density is found once a layer of particles remains in contact or “stuck” to the wall liner.

Once the thresholds have been identified for surface tension and adhesion energy density, from the calibration tests above, an iteration process of parameter sets can be undertaken on the experimental apparatus that was developed in the previous section. The experimental batch rig calibration process will form a database of parameters which can then be scaled to suit on-site applications, in relation to geometry of the plant and run of mine particle sizes. TABLE 2 indicates the parameter sets that was utilised in this research.

RESULTS AND DISCUSSION

The following section contains a summary of the experimental results obtained during the research. In addition, the comparison of DEM to experimental results will be analysed. The summarised results include a description of the identified modes of failure, where a quantitative measure of the recorded impact force and material build-up data was also evaluated.

Experimental Results (Batch Rig)

During the experimental phase of the research, three different modes of failure were identified. These modes included; (1) free flowing, (2) material build-up and break away failure, and (3) material build-up. Each mode of failure is represented in FIG 5 below. It was found that for all three iron ore samples that were tested, with an increase in moisture content an associated increase in the build-up of the sample was experienced. It should be noted, that for different wall lining material no discernible trend was found to the amount of build-up that was experienced. TABLE 3, shows the moisture contents that were analysed for each iron ore sample.

A free flowing failure occurred when a bulk material with lower moisture content was tested. In this case material would impact the impact plate but fail to build-up, flowing over the plate in a consistent stream of material. This mode of failure was identified as a baseline and included for completeness of this paper. Moisture contents that showed these characteristics included Ore A – (8.1% and 9.5%), Ore B – (10.8%) and Ore C – (11.8%). These are typically identified as non-problematic bulk materials. FIG 6 below, is indicative of the transient force response that was recorded during the experimental procedure. Looking at the force response for the free flowing case, it can be seen that a relatively constant impact force is experienced where the initial and final mass both represent zero build-up of the iron ore sample.

The second mode of failure was observed when the bulk material would build-up and break away. This mode of failure most commonly occurred when a bulk material with moderate moisture content was tested. This mode of failure occurs due to the introduction of an adhesive force acting between the wall liner and bulk material. The bulk material build-up would continue until a threshold was met where the adhesive force would fail and the material continues to flow. Moisture contents that showed these characteristics included Ore A –

(10.8%), Ore B – (12.6% and 14.4%) and Ore C – (14.1%). These are typically identified as potentially problematic bulk materials. Failure mode 1 in FIG 6, indicates a potentially problematic sample where the transient force response shows the material build-up until a failure point is reached where a reduction in the force will represent the iron ore sample flowing off the base of the wall liner.

The final mode of failure observed was when bulk materials would build-up and fail to break away. This mode of failure most commonly occurred on iron ore samples that had excessive amounts of moisture content present. The moisture content that showed this characteristic was Ore C – (16.5%). This mode is typically found for bulk materials identified as severely problematic. Failure mode 2 in FIG 6, indicates a severely problematic sample where the transient force response shows the material build-up, where no failure point (reduction in force) is reached. This mode of failure occurs due to the introduction of an adhesive force acting between the wall liner and bulk material.

DEM Comparison

For each of the identified modes of failure above, a DEM comparison could be undertaken where good correlation was found. Similar to the experimental results, where increasing moisture content resulted in an increase in problematic behaviour, an increase in both surface tension and adhesion energy density resulted in a greater build-up of material. Firstly, for the free flowing case a good correlation in the flow of material is seen in FIG 7. This is further justified by examining the force response for the free flowing case, indicated in FIG 8, where it can be seen that a relatively constant impact force is experienced where the initial and final mass both represent zero build-up of the iron ore sample.

The second mode of failure simulated was when the bulk material would build-up and break away. This mode of failure occurred due to the introduction of adhesion energy density between the wall liner and particles. In addition, an increase in the surface tension was added between the particles to achieve this behaviour. Good correlation in the build-up and failure mode of material is seen when FIG 5 and FIG 7 are compared. This is further validated by looking at the transient force response between both the experimental, as indicated in FIG 6, and simulation data found in FIG 8.

The final mode of failure was when the bulk material would build-up and fail to break away. This mode of failure occurred due to the increase of adhesion energy density between the wall liner and particles. In addition, a further increase in the surface tension was added between the particles to achieve this behaviour. Good correlation in the build-up and failure mode of material is seen when FIG 5 and FIG 7 are compared. This is further justified by looking at the transient force response between both the experimental, as indicated in FIG 6, and simulation data found in FIG 8.

When comparing both the experimental data and simulated data, it can be seen that good correlation can be found. With this correlation being found within the database of parameters that has been formed, an adjustment of particle size distribution and geometry can be scaled to simulate what may happen on-site.

CONCLUSIONS

This paper presents a newly coupled contact model into the discrete element modelling (DEM) technique to represent wet and sticky iron ores. The models that were coupled included the Simplified Johnson-Kendall-Roberts (SJKR) contact model, which is an expanded form of the classical hertz model, for particle-to-wall contact. The second part of the model included the EASO liquid bridging model, which accounts for the capillary effects and surface tension that will form between two uneven sized particles such as that of WSM particles. This was included for particle-to-particle contacts. Both of these models were coupled to give the best representation of a WSM, which was simulated using LIGGGHTS (Kloss and Goniva, 2010) as the software platform.

Additionally, this research also investigated the adhesion of problematic iron ore samples onto impact plates under dynamic conditions. An experimental setup consisting of an apron feeder and inclined impact plate was constructed, where three different iron ore samples were tested at three different moisture contents for each sample. This was undertaken for different wall liner materials and wall liner angles where a reduction in wall liner angle resulted in an increase to the amount of build-up that was experienced. For different wall lining material, no discernible trend was found to the amount of build-up that was experienced. Three different modes of failure were identified during the research which included; (1) free flowing, (2) material build-up and break away failure, and (3) material build-up. These modes correlated to an increase in moisture content, where the more moisture that was added to each sample resulted in a build-up of bulk material on the wall liner.

Finally, a series of calibration DEM simulations were undertaken on the experimental setup and particle size distributions (PSD) of the iron ore samples. This series was iterated for the thresholds of surface tension between the particles and adhesion energy density for particle-to-wall contact that were established in the course of the research. The computed database showed good correlation to the experimental results that had been obtained, where all three modes were able to be reproduced within the DEM technique. This can be seen when FIG 5 and FIG 7 are compared. This enabled the formation of a database of parameters, which can be scaled for on-site applications in relation to geometry of the plant and PSDs that would represent run of mine ores.

ACKNOWLEDGEMENTS

The authors wish to acknowledge the Australian Research Council (ARC) Research Hub for Advanced Technologies for Australian Iron Ore, for the assistance given during the research and are grateful for the financial support that has been provided.

REFERENCES

- Burbaum, U, 2009. Adhesion of Cohesive Soils on Material Surfaces of Tunnel Boring Machines. *Darmstadt University of Technology, Institute of Applied Geosciences*.
- Carr, M J, Chen, W, Williams, K and Katterfeld, A, 2016. Comparative Investigation on Modelling Wet and Sticky Material Behaviours with a Simplified JKR Cohesion Model and Liquid Bridging Cohesion Model in DEM.

in *Proceedings 12th International Conference on Bulk Solids Material Storage, Handling and Transport* (Engineers Australia: Barton, ACT).

CFDEM, Gran Cohesion Easo/Capillary/Viscous Model. <http://www.cfdem.com/media/DEM/docu/gran_cohesion_easo_capillary_viscous.html> Retrieved 23 July 2016.

Connelly, D, 2011. High Clay Ores - A Mineral Processing Nightmare, *The Australian Journal of Mining : AJM*. July-August Print Edition. (General Magazine Co.: Richmond North, Vic).

Essington, M, 2003. Soil and water chemistry: A integrative approach (CRC Press: Boca Raton, FL).

Hering, E, Martin, R, and Stroher, M, 1989. *Physics for Engineers* (VDI-Verlag: Düsseldorf).

Hertz, H R, 1896. On the Contact of Rigid Elastic Solids. *Jones and Schott*, pp 156. (Macmillan: London).

Israelachvili, J N, 1992. Intermolecular and Surface Forces. Second ed. (Academic Press: San Diego, CA).

Johnson, K L, Kendall, K, and Roberts, A D, 1971. Surface Energy and the Contact of Elastic Solids. in *Proceedings of the Royal Society of London. Series A. Mathematical and Physical Sciences*, 324(1558): pp 301-313.

Katterfeld, A, Donohue, T J, and Chen, W, 2013. On the Calibration of Bulk Solids for Discrete Element Modelling. in *Proceedings 11th International Conference on Bulk Solids Material Storage, Handling and Transport* (Engineers Australia: Barton, ACT).

Kloss, C and Goniva, C, 2010. LIGGHTS – A New Open Source Discrete Element Simulation Software. in *Proceedings Fifth International Conference on Discrete Element Methods*. pp 25-26. (Springer: Singapore).

Long, J, 2009. Wet and Sticky Ore Mystery... A Thing of the Past? <<http://news.curtin.edu.au/headlines/wet-and-sticky-ore-mystery-a-thing-of-the-past/>> Retrieved 12 January 2016.

Rabinovich, Y I, Esayanur, M S, and Moudgil, B M, 2005. Capillary Forces between Two Spheres with a Fixed Volume Liquid Bridge: Theory and Experiment. *Particle Engineering Research* (University of Florida: Gainesville, FL 32611).

Roberts, A W, 1998. Basic Principles of Bulk Solids, Storage, Flow and Handling, *Centre for Bulk Solids and Particulate Technologies* (The University of Newcastle: Callaghan, NSW).

Rumpf, H, 1958. Principles and Methods of Granulation. *Chemical Engineering and Technology*, 30(3): pp 144-158.

Soulié, F, Cherblanc, F, El Youssoufi, M S and Saix, C, 2006. Influence of Liquid Bridges on the Mechanical Behaviour of Polydisperse Granular Materials. *International Journal for Numerical and Analytical Methods in Geomechanics*, vol. 30, pp 213-228.

FIGURES

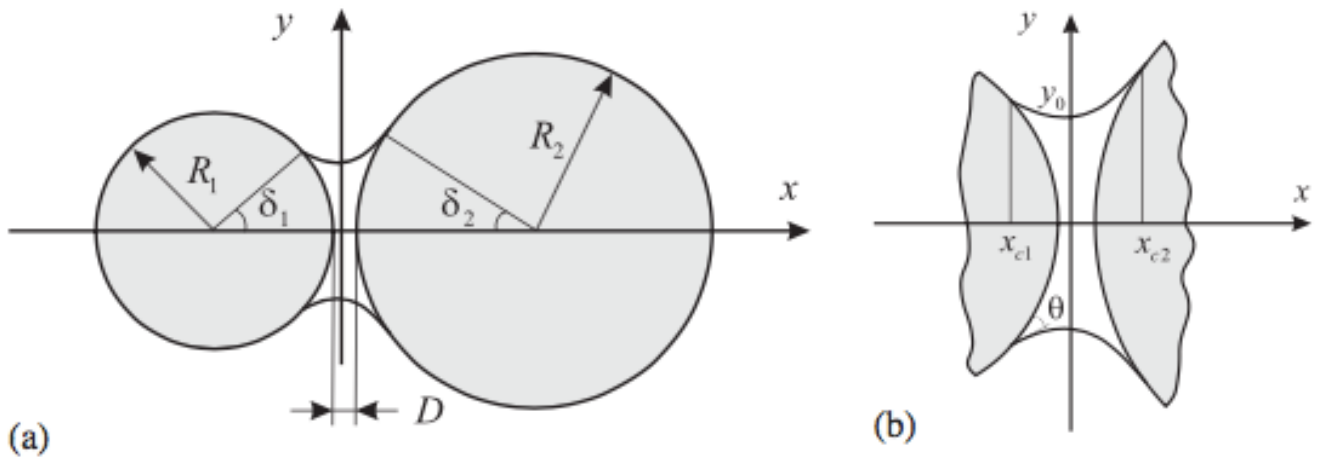


FIG 1 – (a) Geometry of a liquid bridge between two particles of uneven sizes. (b) Detailed view of liquid bridge (Soulié, 2005).

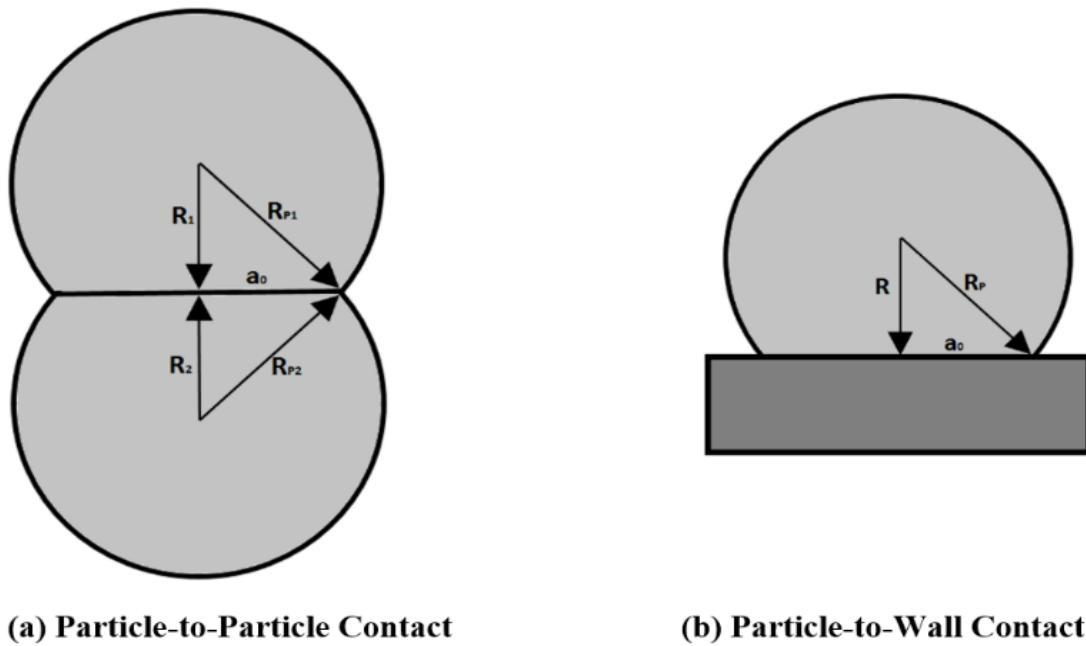


FIG 2 – Schematic of the SJKR contact model (Chen, 2015).



FIG 3 – Experimental apparatus.

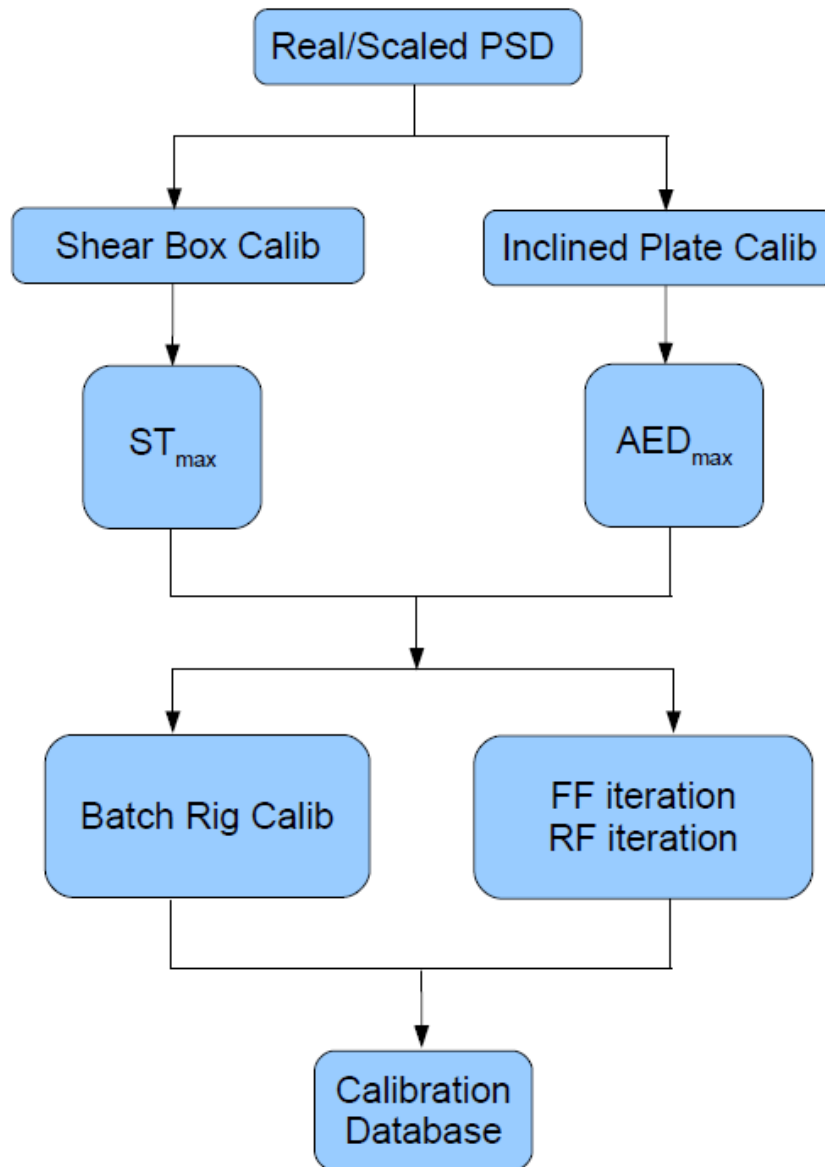


FIG 4 – DEM calibration flow chart.



FIG 5 – Experimental impact testing modes of failure.

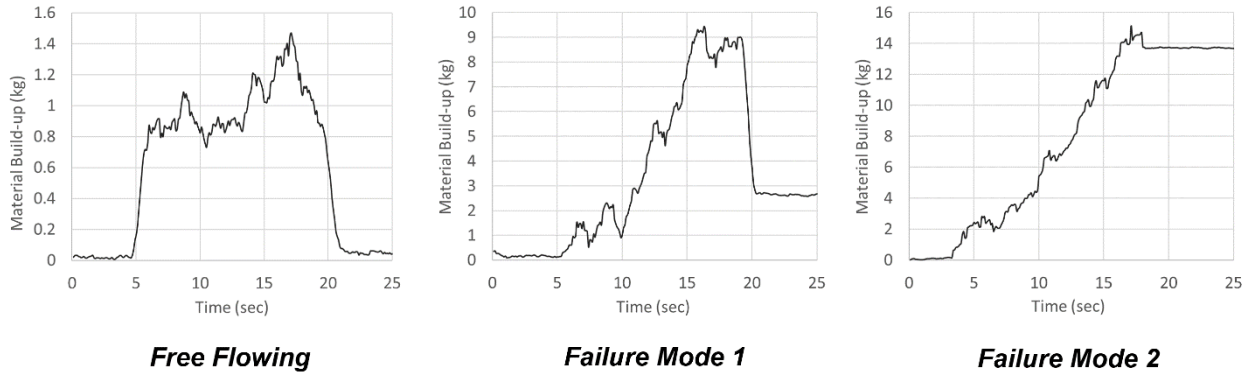


FIG 6 – Experimental impact testing transient force response for different modes.

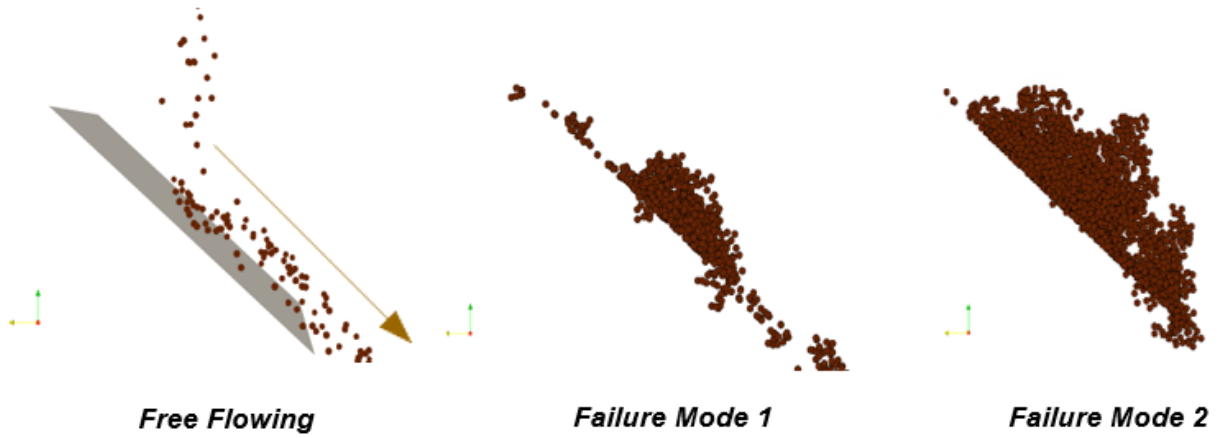


FIG 7 – Impact testing modes of failure DEM prediction.

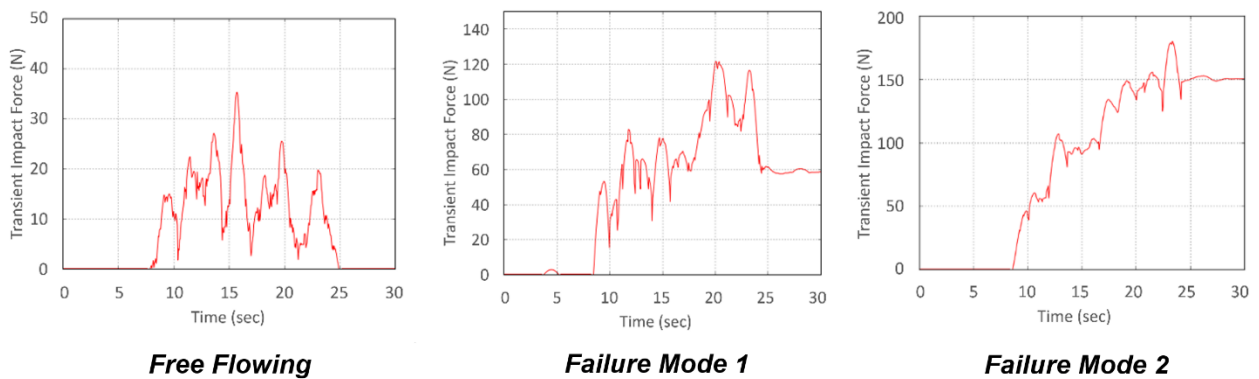


FIG 8 – Impact testing transient force response DEM prediction for different modes.

TABLES

TABLE 1

Experimental Variables

Assessable Variables	Constant Variables
<i>Iron Ore Samples</i>	<i>Mass Flow Rate</i>
<i>Moisture Content</i>	<i>Impact Height</i>
<i>Impact Angle</i>	<i>Conveyor Velocity</i>
<i>Wall Lining Material</i>	

TABLE 2

DEM Parameter Iteration Sets

DEM Parameter	Parameter Iteration
<i>Surface Tension (ST)</i>	<i>0 : 5 : 20 [N/m]</i>
<i>Adhesion Energy Density (AED)</i>	<i>0 : 5e⁴ : 25e⁴ [J/m³]</i>
<i>Particle Friction (FF)</i>	<i>0.1 : 0.1 : 0.9</i>
<i>Rolling Friction (RF)</i>	<i>0.1 : 0.1 : 0.9</i>

TABLE 3

Iron Ore Sample Moisture Contents

Sample ID	Moisture Content
<i>Ore A</i>	<i>8.1%, 9.5%, 10.8%</i>
<i>Ore B</i>	<i>10.8%, 12.6%, 14.4%</i>
<i>Ore C</i>	<i>11.8%, 14.1%, 16.5%</i>